Novel Genetically Optimised High-Displacement Piezoelectric Actuator with Efficient Use of Active Material

Katja Poikselkä[1], Mikko Leinonen[2], Jaakko Palosaari[2], Ilari Vallivaara[1], Juha Röning[1] and Jari Juuti[2]

[1] Department of Computer Science and Engineering, University of Oulu, Erkki Koiso-Kanttilan katu 3, 90570 Oulu, Finland
[2] Microelectronics Research Unit, University of Oulu, Erkki Koiso-Kanttilan katu 3, 90570 Oulu, Finland

Corresponding author: Katja Poikselkä
Email: katjalut@gmail.com

This paper introduces a new type of piezoelectric actuator, Mikbal. The Mikbal was developed from a Cymbal by adding steel structures around the steel cap to increase displacement and reduce the amount of piezoelectric material used. Here the parameters of the steel cap of Mikbal and Cymbal actuators were optimised by using genetic algorithms in combination with Comsol Multiphysics FEM modelling software. The blocking force of the actuator was maximised for different values of displacement by optimising the height and the top diameter of the end cap profile so that their effect on displacement, blocking force and stresses could be analysed. The optimisation process was done for five Mikbal- and two Cymbal-type actuators with different diameters varying between 15–40 mm. A Mikbal with a Ø 25 mm piezoceramic disc and a Ø 40 mm steel end cap was produced and the performances of unclamped measured and modelled cases were found to correspond within 2.8 % accuracy. With a piezoelectric disc of Ø 25 mm, the Mikbal created 72 % greater displacement while blocking force was decreased 57 % compared with a Cymbal with the same size disc. Even with a Ø 20 mm piezoelectric disc, the Mikbal was able generate ~10 % higher displacement than a Ø 25 mm Cymbal. Thus, the introduced Mikbal structure presents a way to extend the displacement capabilities of a conventional Cymbal actuator for low-to-moderate force applications.

Keywords: genetic algorithm, optimisation, piezoelectric, Mikbal, Cymbal, actuator

Introduction

Actuators that generate force and displacement are the basis for a wide range of industrial and consumer products that provide regulation, on-off motion or continuous operation. Actuators are an essential part of these devices and an important aspect in improving their performance. Examples include diesel injection systems in automobiles or accurate alignment of mirrors in optical applications [1-2]. Piezoelectric materials exhibit an exceptionally compact structure, extreme resolution and low response time, among other required properties. However, they fall short in displacement, as typically these materials exhibit strains in the order of 0.1–0.2 %. To overcome this shortage, dozens of different methods for extending operational displacements have been applied, employing internal and external leverage methods. Internally leveraged actuators rely on stacks or bending of piezoelectric actuator structures, as in the case of unimorphs, bimorphs, monomorphs and their derivatives. In such cases, straining of the piezoelectric material in an electric field is amplified by bending the structure at the cost of decreased force generation capabilities. [3]

To expand the range of applications of piezoelectric devices even further, components providing moderate load-bearing capability are needed. Internally leveraged actuators typically exhibit the highest displacements within the smallest volume; however, their downfall is low generated forces. Therefore, externally leveraged actuators utilising hydraulic systems, levers or Moonie/Cymbal-type structures (i.e., bending of the external structure) and producing moderate forces and also high displacements with small volume are required. [3] In addition, decreased volume in piezoelectric ceramics would be preferred as they tend to be relatively expensive compared with common passive materials like plastics or metals. In the case of the widely studied Cymbal actuator, bending of the end cap on both sides of the piezoelectric sheet is utilised to create high displacements and moderate forces. This structure is very compact and has offered a wide range of adjustability for numerous different applications. [3] In the past, Cymbal transducers have been optimised for various cases. Very recently, for

example Sheng *et al.*, optimised the shape of a Cymbal stack transducer with FEM modelling and a zero-order method to improve the generated displacement even further [4]. Also Huan *et al.* studied the effect of changing different parameters of a Cymbal to increase displacement and frequency for a drug delivery application [5]. In addition, Narayanan *et al.* presented a Cymbal with radial holes called a Wagon Wheel, which decreases tangential stresses and amplifies the displacement produced by the Cymbal [6]. Also the effect of different ceramic driving elements to the displacement of the Cymbal actuator have been studied by Ngernchuklin et al. [7].

While a number of different approaches have been used to optimise Cymbal transducers, a genetic algorithm (GA) has not been applied until very recently [8]. A genetic algorithm is a stochastic optimisation method that has gotten its inspiration from the evolution of nature. In a GA, a whole population of solutions is optimised at the same time. The fitness of the solutions is estimated and utilised when solutions are combined and mutated to produce a new population. After multiple iterations, the population of solutions has evolved. Genetic algorithms are suitable for solving complicated, multidimensional optimisation problems and thus they are a good choice for optimising the structural parameters of the new piezo actuator model.

Genetic algorithms have been used widely in the field of material technology, for example, in MEMS design [9-11], prediction of a stable crystal structure of a compound [12], the design of flat structures for vibration suppression [13] and optimal design of an optical image stabiliser mechanism for cameras in mobile phones [14].

Genetic algorithms have also been utilised in designing a piezoelectric forceps actuator [15], optimising a surgical ultrasonic piezoelectric transducer [16], composite structural optimisation problems [17-19], designing a star-shaped flextensional stator [20], optimal placement of piezoelectric actuators in vibration control [21], topology design of large displacement compliant mechanisms [22] and optimising the design parameters of a Cymbal actuator [8].

In earlier experiments a GA has proved to be a very powerful tool in optimising a Cymbal structure. In this paper a GA is applied to a new structure called Mikbal which is derived from a Cymbal actuator. The purpose of the new design is to lower the amount of PZT material and still get high displacements compared to Cymbal actuator. This will enable more efficient utilisation of the active PZT material and facilitates also the use of not so common or more expensive materials like single crystal PMN-PT.

The GA was used to optimise the parameters of the steel end cap of a Mikbal-type actuator to achieve specified displacements with maximal blocking force for each displacement. The optimisation was repeated for multiple discrete values of displacements to get curves as a function of displacement. The process was done for five different Mikbal-type actuators and two Cymbal-type actuators with different steel thicknesses. The Mikbal structure with a steel thickness of 250 µm was produced and displacement was measured and compared with simulation results.

1. Design

The purpose of the actuator design was to achieve a structure that uses less active material than traditional Cymbal actuator of the same size. Piezo volume can be lowered by using thinner discs or by changing the radius of the disc. In the case of a Cymbal actuator, material thinning can be done easily, but the change in radius requires a completely new design, provided that the overall diameter of the actuator is kept the same. In this work, some of the piezo material is substituted by using thin steel flanges at the outer rim. These flanges are then connected to the end caps as shown in Fig. 1. The motivation of this design, called Mikbal, is to use the larger steel structure as leverage for the smaller piezo layer. In the traditional Cymbal, when using a small-diameter piezo disc the end cap design is also scaled down simultaneously, decreasing also the leverage it provides. The Mikbal compensates the smaller piezo layer with a larger steel structure, which thereby generates higher displacement amplification.

In a Cymbal structure, the outer rim of the end cap is glued directly to the piezo layer and therefore cannot bend at the edge (Fig. 1a). In this new design, the end caps are glued into flanges which can bend at the edges toward each other. This bending limits displacement, as can be seen in later chapters, and has to be minimised. Various supporting structures that provide adequate support for the end caps are discussed in this paper. This new structure has a number of parameters that need to be optimised. Some of them are the same as in traditional Cymbals, such as the shape of the end caps and the thicknesses of the piezo layer and the end caps. However, some new parameters are introduced in this new actuator. These include the thicknesses of the steel flanges and also the glue

area between the flange and the piezo layer.

The model of the Mikbal-type actuator was defined as a parameter vector [h, d, d_{top},d_{pzt}, W_e,W_s, P_Z, P_S, V] (Fig.1b). The fixed parameters, i.e. not variables, were the total diameter d at 40 mm, the width W_e and thickness of the gluing surface of 1.5 mm and 0.1 mm, respectively, piezo thickness P_Z of 1 mm, steel thickness P_S of 0.25 mm and the electric field of 1 kV/mm. The thickness of the flange was 0.1 mm and it was glued at a width W_s of 1.5 mm onto the surface of the piezo material. To enable comparison, the fixed parameters were selected based on previous results [8]. For both Mikbal and Cymbal actuators, the output point for displacement and force d_{top} and the height of the air gap h were free variables. The optimisation process was done with piezo disc diameters of 25 mm and 40 mm; and 15 mm, 20 mm, 25 mm, 30 mm and 35 mm (d_{pzt}); for Cymbal and Mikbal, respectively. The same material parameters were used for PZT and steel as in the authors' previous studies [8]. These parameters are shown in Tables 1 and 2 with the addition of the epoxy glue used in the end cap support and the plastic pads at the top and bottom.

Table 1. Piezo material properties used in the FEM simulations.

PZT-5H	Elastic compliance ($1x10^{-12}$ m^2/N)	$S^E_{11,22}$	16.5
		$S^E_{12,21}$	-4.78
		$S^E_{13,23,31,32}$	-8.45
		S^E_{33}	20.7
		$S^E_{44,55}$	43.5
		S^E_{66}	42.6
	Piezoelectric charge coefficient ($1x10^{-12}$ C/N)	$d_{31,32}$	-274
		d_{33}	593
		$d_{15,24}$	741
	Relative permittivity	$\varepsilon_{11,12}$	3130
		ε_{33}	3400
	Density (kg/m^3)	ρ	7500

Table 2. Material properties for passive materials.

	Young's Modulus (GPa)	Poisson's ratio	ρ (kg/m^3)
Steel	200	0.33	7850
Epoxy	3.9	0.3	1183
Pad	2	0.4	1150

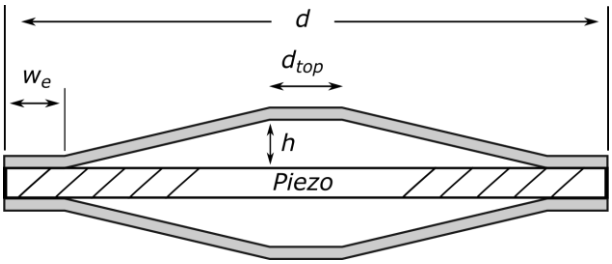

Figure 1a. Cross-section schematic of a Cymbal and used parameters.

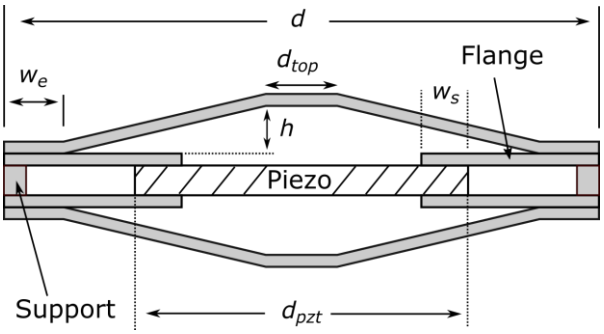

Figure 1b. Cross-section schematic of a Mikbal actuator and the parameters used.

2. Modelling

Cymbal- and Mikbal-type piezoelectric actuators were modelled using FEM (Finite Element Method) software (COMSOL Multiphysics 4.3a, COMSOL AB). Displacement and blocking force simulations were carried out. Both of these simulations were static linear simulations. Since the device under study was an actuator generating relatively small deformations, a linear simulation type was selected. The boundary conditions for the displacement simulations were: the bottom of the end cap, or the area defined by d_{top}, was fixed and the top of the end cap was therefore able to move freely. For the blocking force simulations, the positions of both the top and bottom end caps were fixed and the force generated by the actuator was recorded. The ideal clamping condition i.e. mathematical constraint at the edge of the flanges were applied, to keep the distance between the top and bottom end cap edges constant, while not restricting the bending of the structure. Automatic meshing was done using triangles, seen in Figure 2, at every simulation. The simulated elements were quadratic Lagrange elements. The geometry was modelled using a 2D axial symmetric model, which enabled fast simulations as opposed to using a 3D model. The speed of simulation was an important factor, since a genetic algorithm requires a large amount of simulations.

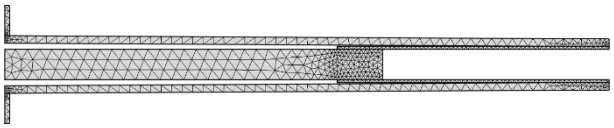

Figure 2. The meshed axial symmetric model.

The optimisation was done with a genetic algorithm with the optimisation tool of Matlab (R2012b). The population consisted of parameter sets for piezo actuators. The parameters (genes) of the Cymbal and Mikbal models were the height and diameter of the top region, so the chromosome was [d_{top}, h]. Different Cymbal models had different diameters (25 mm and 40 mm). The total diameter of all Mikbal models was 40 mm and the length of the piezo diameter varied between 15 mm and 35 mm.

Figure 3 represents the optimisation process of an actuator. Specifications and the model are given to genetic algorithm which utilises FEM modelling and optimises given parameters of the model.

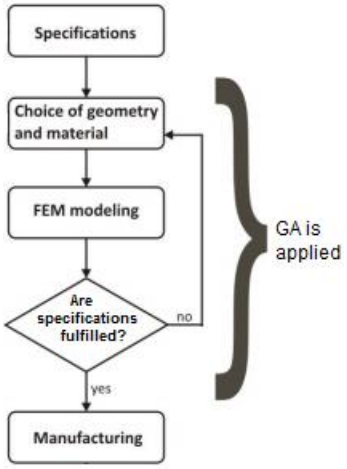

Figure 3. The optimisation process.

The optimisation proceeded so that displacement was forced into a specified value with the fitness function while the blocking force was maximised. This was done for discrete values of displacement to get the maximum blocking force as a function of displacement, which enabled presentation of all properties as a function of displacement. The optimisation process was repeated seven times in total, for five different models of the Mikbal actuator and for two different models of the Cymbal actuator. The fitness function was

$$y = (1 + (s_0 - s)^2)/F \qquad (1)$$

where s_0 is the desired displacement, s is FEM-modelled displacement and F is the blocking force. A power of two was used to make the effect of the displacement term stronger, since force tends to dominate the fitness function very strongly. There is a natural trade-off between force and displacement, thus a smaller displacement typically means a larger generated force. The calculated fitness value for each individual was scaled based on its ranking in fitness. An individual with rank r has a scaled score proportional to 1/sqrt(r). This helped the population preserve its diversity when only a few very good solutions were found. A population size of 50 and 70 generations were used. The simulations were done with blocks of 10 individuals to save time. The simulation of one individual took about 21 seconds, making the computation time for one evolutionary run circa 21 hours.

The two best solutions of the population were delivered to the new generation as elite individuals to preserve found solutions. Of the remaining individuals in the new population, 40 % were produced with mutation and 60 % with crossover. Parents were selected deterministically based on the integer part of the scaled score of their fitness and roulette selection was used on the remaining fractional part. Gaussian mutation with deviation less than 25 % of the searching range in the beginning of the evolution was used. During the evolution, the amount of mutation was decreased linearly so that in the end it was less than 1 % of the searching area. In the beginning individuals were able to travel to the opposite side of the searching area in a few generations but they were not spread around the space in every mutation. The contradiction of the mutation made the local search for the GA easier after the population was converged near the best solution the GA had found. The mutation was also modified to stay inside of given boundaries of height and top diameter. The boundaries of the parameters covered about a 1 mm range in the height h and a 3–5 mm range in the diameter of the cap d_{top}, whereas the starting point was defined by the solutions found earlier.

The crossover function created offsprings by a random weighted average of the parents with a ratio of 1.1. Thus the individuals of the new generation had properties between their parents with a high possibility, but they also had a chance to spread outside of the space defined by the genes of the parents, which helped the population preserve its diversity. Same parameters of the GA were used in [8]. The GA provided good results and there was high similarity in the results of separate but identical evolutionary runs and therefore no effort was made to optimise the parameters of the GA further.

3. Experiments

A Mikbal-type actuator was manufactured for measurements. The steel end caps (Ø 40 mm, 250 µm thick) and flanges (Ø 40 mm, inner Ø 22 mm, 100 µm thick) were laser-machined (Siemens Microbeam 3200, Siemens AG). Two piezoelectric discs with silver electrodes (PZT-5H, Ø 25 mm, 500 µm thick) were glued (Loctite 401 fast glue, Henkel Corp.) together and a small drop (Ø 2 mm) of conductive silver paint was added to the glue to ensure good electrical contact. Flanges were then glued (Strong Epoxy Metal 2810, Casco) from the inner perimeter onto both sides of the piezoelectric discs at a 1.5 mm distance. Subsequently, end caps were glued (Epoxy) to the flanges at a 2.0 mm distance from the outer perimeter of the flanges. Small holes (Ø 0.5 mm) were micro-machined around the outer perimeter of the end caps to ensure robust contact with the flanges and the end caps. A hydraulic press was used to compress the end caps slightly to a dome shape, which created a ~650 µm air gap between the piezoelectric disc and the end cap. The shape of the steel end caps was measured using a micrometre screw (Mitutoyo Coolant Proof IP65, USA). The shaping of the end caps was done to provide an initial preferred bending direction for the end caps. Obviously, this slightly reduces displacement.

Actuator (Fig. 4) displacement was then measured as a function of electric field (sine wave at 0.5 Hz) with a fibre-optic laser vibrometer (OFV-5000, Polytec GmbH). The first measurement was done without support between the end caps, the second measurement with 8 small (Ø 2 mm) epoxy pillars between the end caps at the outer perimeter and the third measurement with 16 supporting pillars. Displacement was measured from the middle point of the actuator, which was glued on a Ø 5 mm pedestal from the opposite side. The measurement system is represented in Fig. 5.

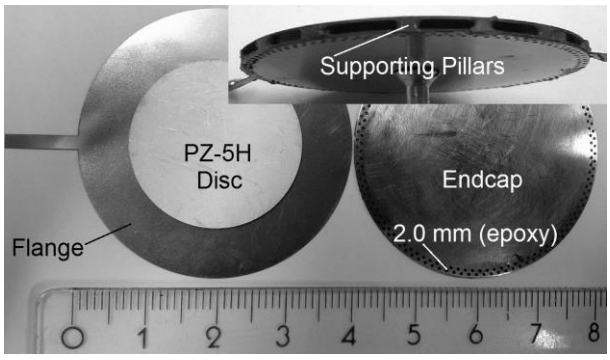

Figure 4. Assembled Mikbal actuator.

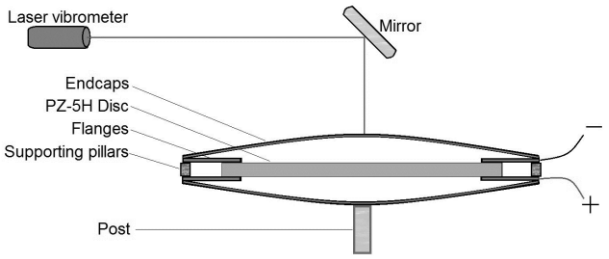

Figure 5. Displacement measurement of the actuator.

4. Results

In the figures below, simulated data points are plotted as a function of displacement. Every point is a result of the optimisation process done with the genetic algorithm, exhibiting the actuator with the highest figure of merits. These points are plotted and analysed with respect to blocking force, von Mises stress and optimised height and top diameter values.

Fig. 6 shows the maximum obtainable blocking force (within the computation time used) as a function of displacement for different Cymbal and Mikbal actuators (note the logarithmic scale).

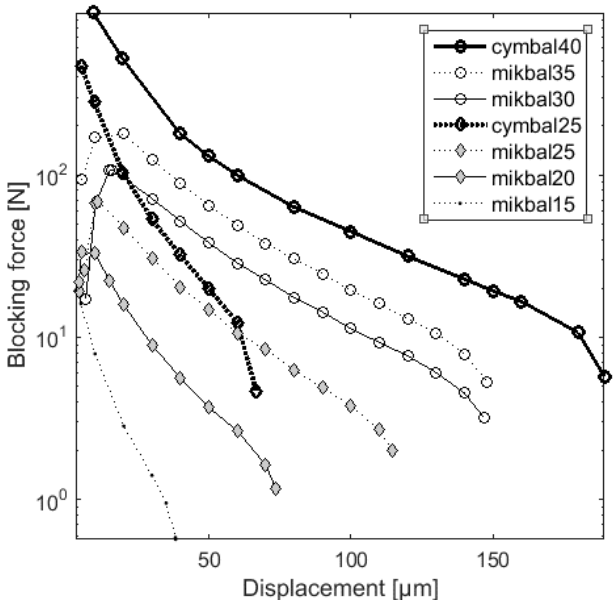

Figure 6. Blocking force as a function of displacement.

It can be seen that Cymbal actuators give a significantly higher blocking force than Mikbal actuators when small displacement capabilities are allowed. In contrast, when higher operational displacement is required, Mikbal outperforms Cymbal, achieving also a higher blocking force in the high displacement region (e.g., above 60 µm in the case of Mikbal25 and Cymbal25). It can be

noticed that the region of rapid decrease in blocking force at the end of the graphs in Fig. 6 is moved towards higher displacements in the case of Mikbal. This is the result of an improved displacement generation capability due to additional flanges. The ending point of each curve is defined by the highest produced displacement and the corresponding blocking force that can be generated by that structure. Reaching lower blocking forces than those shown here was not possible for these structures with the fitness function we used where the force was maximised.

In Fig. 6 the largest displacements were achieved with a Ø 40 mm Cymbal, as the outer diameter of the Mikbal was limited to Ø 40 mm, in which cases flanges would not exist. However, a Mikbal actuator with a piezo disc of Ø 20 mm seems to be already capable of generating a higher displacement than a Cymbal of Ø 25 mm, but with a lower blocking force. Moreover, with the same size piezo, Mikbal25 is able to generate a ~72 % higher displacement than Cymbal25. Therefore, the structure of a Mikbal actuator is especially beneficial in applications where extension of the displacement range is required. It is also clear from Fig. 6 that displacement increases rapidly with larger size piezo discs. This observation is more visible in Fig. 7. where also saturation of displacement at a piezo size of Ø 30 mm is shown. At the same point the blocking force is rapidly increased, thus the structure is switching from displacement amplification more towards force generation as a consequence of the dimensional ratios of the flange and the piezo disc. Thus, for each selected size of the piezo, optimal flange dimensions should be found. In this case with the outer diameter set to Ø 40 mm, the optimal flange width would be 7.5–5.0 mm for a Ø 25–30 piezo, respectively, corresponding to a ratio of 3:5–1:3 between flange width and piezo radius.

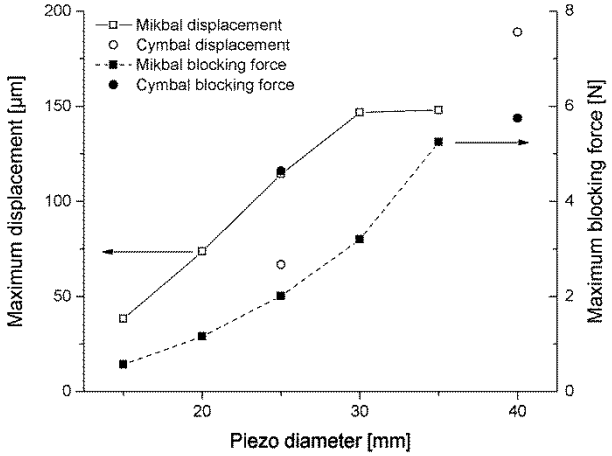

Figure 7. Maximum displacement and related blocking force of a Mikbal actuator as a function of the diameter of the piezo disc.

It should also be noted that each Cymbal actuator presented here is highly optimised by the GA presenting the best structure, within the same boundary conditions as the Mikbal actuators, and therefore should give a generic understanding about obtainable performance. The numerical values of the dimensions and performance of the Cymbal and Mikbal actuators are gathered into Table 3. From this Table it is evident that a Cymbal is the more preferable structure when higher forces are required (466.5–992.3 N) while a Mikbal generates higher displacements with the same size piezo.

Table 3. Blocking force and displacement at maximum displacement and maximum blocking force as a function of piezo and total diameter for Cymbal (C) and Mikbal (M) actuators.

Actuator type	**M 15**	**M 20**	**M 25**	**C 25**	**M 30**	**M 35**	**C 40**
Piezo dia.[mm]	15	20	25	25	30	35	40
Total dia.[mm]	40	40	40	25	40	40	40
At maximum displacement							
Disp. [µm]	38.3	73.6	114.4	66.7	146.8	148.0	189.1
Max force [N]	0.6	1.2	2.0	4.6	3.2	5.3	5.8
At maximum blocking force							
Disp. [µm]	3.1	5.2	11.0	5.1	15.8	20.0	9.3
Max force [N]	19.5	33.7	68.8	466.5	107.5	178.4	992.3

From Fig. 8 it can be seen that a Mikbal-type actuator has lower maximum Von Mises stress than a Cymbal actuator. The length of the steel end cap is much greater for a Mikbal than for a Cymbal, taking into account also flanges. Therefore, the second moment of inertia and stiffness of the end cap structure is less than in Cymbals, causing decreased resistance of the piezo movement and thus reduced stresses. Moreover, the stresses were

significantly below the 75 MPa reported as the modulus of rupture for PZT in the transverse direction [23]. Only a ∅ 35 mm Mikbal has slightly higher Von Mises stress than a Cymbal with a 25 mm diameter in large values of displacement. The maximum Von Mises stress of a Cymbal slowly decreases as a function of displacement, but for Mikbals it fluctuates at smaller displacements.

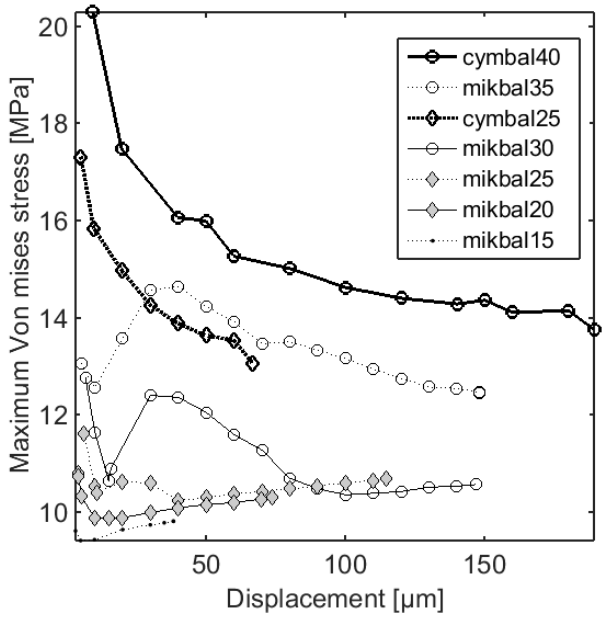

Figure 8. Maximum Von Mises stress of the piezo material as a function of displacement.

It was also observed that for Mikbal actuators, the maximum blocking force (Fig. 6) is typically achieved before the point of highest stresses (Fig. 8). This indicates that the mechanism first reaches its optimal force delivery conditions from the piezo, after which the force becomes more directed into the end cap structure itself rather than the output of the actuator.

Fig. 9 presents the optimal height of the steel cap as a function of displacement for different actuators. The shape of the function is decreasing and quite similar for both Mikbal- and Cymbal-type actuators. However, in the Mikbal the height of the cap is generally smaller than in the Cymbal, especially with large values of displacement. Mikbal-type actuators produce displacement by using the lower end cap, in which case displacement amplification from the horizontal plane (Fig. 1) to vertical motion is the highest. Moreover, flanges provide additional leverage for the structure, but to maximise the blocking force at the same time, some degree of structural rigidity is required by increasing the height of the end cap. The Mikbal increases the height of the end cap significantly when approaching smaller displacement and higher blocking forces. However, it still produces significantly lower blocking forces than the Cymbal and therefore is especially feasible in applications requiring a very low profile and high displacements but moderate forces.

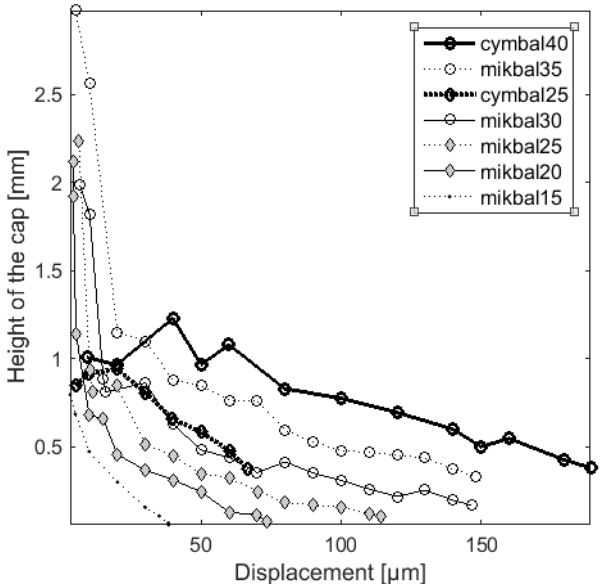

Figure 9. Height of the cap as a function of displacement.

A comparison of Fig. 8 and 9 reveals that together with decreased stresses in the low displacement region, also the height of the end cap is dramatically decreased. In such a case the stiffness of the end cap against bending is greatly decreased, which can be seen as less resistance towards piezoelectric action. Once the most dramatic changes have been passed in the height of the end cap, stresses increases rapidly and then start to decline again. Here, the operation "mode" of the mechanism is changed (low end cap with a small flat region, Figs. 9 and 10) compared with a low displacement region (high end cap with a large flat region), thus causing corresponding changes in movement resistance and stresses of the piezo.

Fig. 10 shows the top diameter of the cap as a function of displacement for different actuators. The shapes of all the curves are linearly decreasing, but the curves for the Mikbals have a steeper slope than the curves for the Cymbals. Also, while the curves for the Cymbals are a little concave, the curves for the Mikbals are more convex. Both the Mikbal and Cymbal actuators reduce the top diameter when aiming for larger displacements and give maximal displacement when the top diameter approaches zero. Shortening the top diameter extends the available lever that can be utilised by the piezo structure. Thus the genetic algorithm minimises the top diameter to reach the required displacement, after which the residual of the flat

region is used to improve force generation.

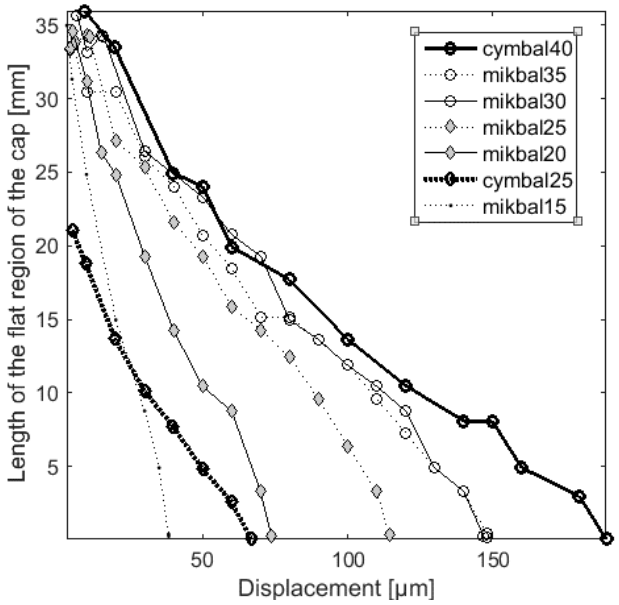

Figure 10. Length of the top diameter of the cap as a function of displacement

Also from Fig. 10 it can be seen that the effectiveness of the Mikbal saturates at ∅ 30 mm since the curves of Mikbal30 and Mikbal35 are mostly overlapping. This was also concluded in the case of Fig. 7.

Table 4 demonstrates the displacement of the structures versus volume of piezoelectric material. Here the advantage of the steel structures of the Mikbal over the Cymbal is clearly seen. With a piezo diameter of 25 mm the Mikbal generates 1.7 times greater displacement than the Cymbal and therefore provides higher efficiency in terms of PZT volume. The Wagon Wheel actuator previously developed by Narayanan *et al.*, i.e., a Cymbal with radial holes [6], achieves values between a Cymbal and Mikbal with a diameter of 25 mm. The highest displacements per amount of piezo material are produced by Mikbals with piezo diameters of 20 mm and 25 mm. The benefit created by the additional steel structures of the Mikbal decreases at around a 30 mm diameter. At this point, although the piezo diameter is increased, it also approaches the total diameter, thus shortening the lever created by the flange and at the same time increasing the amount of piezo material, resulting in lower displacement vs. PZT volume ratio.

Table 4. Maximum displacement with respect to the amount of piezo material.

Actuator	Max displacement / volume of PZT material [µm/mm^3]
Cymbal 25	0.136
Cymbal 40	0.151
Mikbal 15	0.217
Mikbal 20	0.234
Mikbal 25	0.233
Mikbal 30	0.208
Mikbal 35	0.154
Wagon wheel 25	0.187

The manufactured prototype was also modelled with FEM. As the end caps of the manufactured prototype deviated from the ideal GA-simulated model, a new model was developed incorporating the produced end cap design. The curvature of the prototype's end cap was measured and applied to the model. The model allowed us to study the influence of different clamping and supporting methods at the outer rim of the Mikbal. Different support structures were also applied to the prototype and displacement measurements were carried out to compare the results with the modelled results. The measurements and modelling results are shown in Fig. 11. Every point in figure 11 is an average of 5 measurements with the standard deviation 0.1 µm.

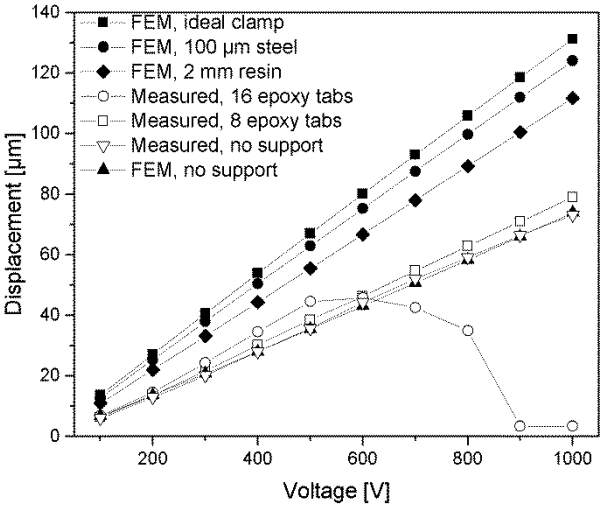

Figure 11. Displacement as a function of voltage with different outer rim clamping methods.

Amount of epoxy on the edges of the actuator was varied by 8 and 16 tabs, and also a case without any support was measured. These tabs are seen in Fig. 1b. As the modelling was carried out as axial symmetric simulations, it was not possible to add discrete tabs. As a result, the effect of epoxy support was simulated using a continuous ring of epoxy at the outer rim of the actuator, as seen in Fig. 12. Simulated cases included the epoxy ring, a no

support case, a 100 µm steel ring and an ideal clamping case. Without any clamping, as seen in Fig. 12, the end of the end caps can bend toward each other and therefore the total displacement is less than in the ideal case. The ideal clamping condition includes a mathematical constraint at the edge of the actuator, which keeps the distance between the top and bottom end cap edges constant, but does not restrict bending. A practical approximation of this condition was modelled with a 100 µm steel strip between the edges. This keeps the distance between end cap ends close to constant. Furthermore, the thickness of 100 µm was selected to allow bending of the end cap and to keep radial stress induced by the clamp minimal as it counters the piezoelectric radial force. This means that if wide and stiff material is used as the support, the resulting ring opposes radial contraction of the piezoelectric disc, thus limiting displacement.

The results in Fig. 11 confirm that the ideal clamp is indeed superior to all of the other support methods. However, the steel rim clamp is very close to the ideal clamp, as was expected. The epoxy rim also provides high performance, but still noticeably lower than the steel rim solution. The best measured case was the 8 tabs version, but as can be seen, the 16 tabs version starts to perform better at lower voltages but then performance suddenly drops. This was due to the prototype breaking. The cause of the fault remained unclear. However, one could argue that by adding more glue tabs, performance would eventually approach that of the epoxy rim case. Finally, the performances of both the measured and modelled unclamped cases were almost identical and their curves in Fig. 11 are greatly overlapping. The results show that utilisation of the correct support or clamping at the edges has a crucial role in this type of actuator, as displacement performance approximately doubles by using an ideal clamp compared with the unsupported case.

Stress distribution under 500 V excitation is shown in Fig. 12. As can be seen, the ideal clamp allows bending of the flanges and the end caps and maximum stress is located at the flanges. In the steel rim case, maximum stress is now located at the rim, but the flanges and end caps are allowed to bend. In the case of the epoxy ring, the axially thick epoxy ring prevents bending of the flanges and also hinders bending of the end caps. This can be seen as a build-up of stress at the end caps near the epoxy ring.

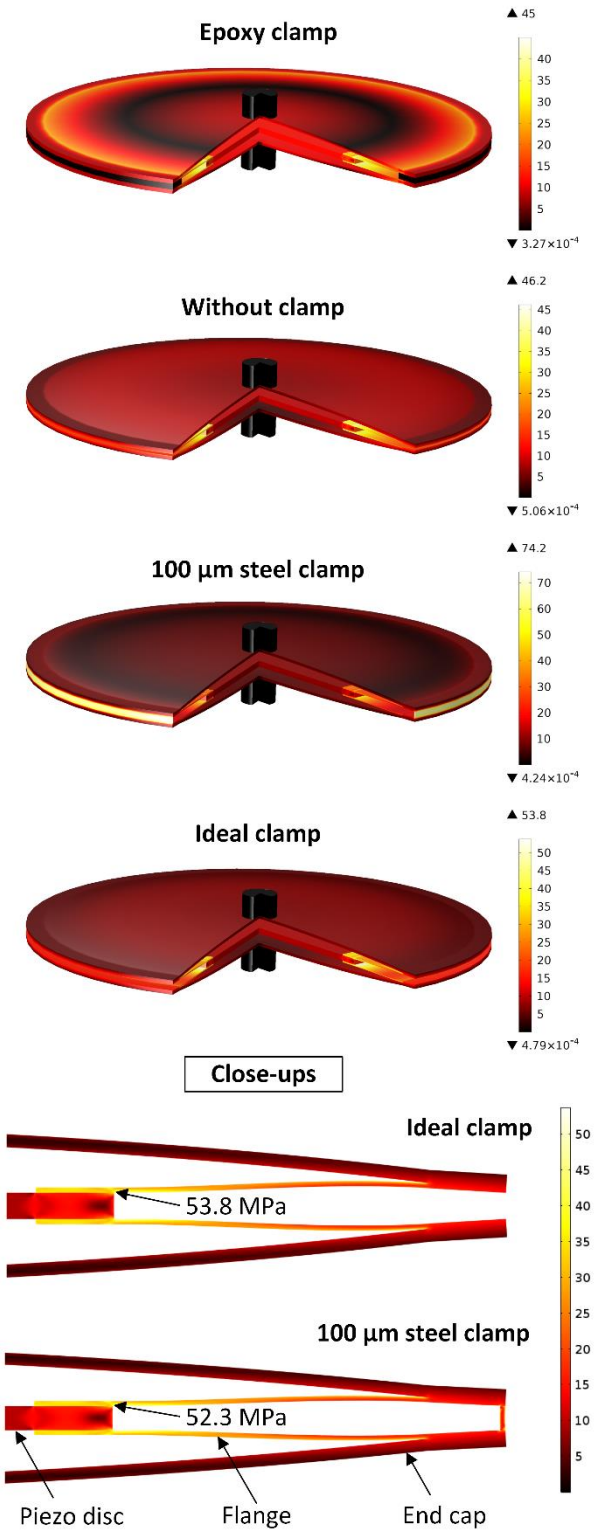

Figure 12. The von Mises in MPa and deformations of the structure under 500 V with different clamps and close-ups of ideal and 100 µm steel clamps.

5. Conclusion

In this study a new modification of the Cymbal-type actuator, called the Mikbal, was modelled and produced. The Mikbal has supplementary steel

structures around it to amplify displacement, which creates larger displacement than the Cymbal with the same amount of piezo material, but gives generally smaller blocking forces.

The parameters of the Mikbal, as well as its Cymbal counterparts, were optimised by a genetic algorithm. An optimised ∅ 40 mm Mikbal steel structure has a ∅ 20–25 mm piezo disc inside and a lower cap than corresponding Cymbal actuators. Lowering the cap and shortening the top region of the end caps of Mikbal and Cymbal actuators increased the generated displacement in both cases.

It was also concluded that the support structure that keeps the distance between the top and bottom end cap edges constant in the perimeter of the Mikbal has a crucial role in its performance. In the case of ideal mathematical constraint the Mikbal generated about twice as much displacement compared with a case without support. For practical realisation also epoxy and a 100 µm wide and thick steel ring were tested, where a steel strip between the edges gave higher performance close to ideal. Furthermore, the measured Mikbal actuator and modelled unclamped cases showed very high correspondence. This paves the way for further improvements by utilising FEM modelling and genetic algorithms and opening some of the constraints from the parameter space used.

Acknowledgement

The authors gratefully acknowledge funding by the Academy of Finland for the Evolutionary Active Materials Project (no. 140410). Author Jari Juuti acknowledges funding by the Academy of Finland (project numbers 273663 and 267573).

References

[1] MacLachlan BJ, Elvin N, Blaurock C and Keegan NJ (2004) Piezoelectric valve actuator for flexible diesel operation. In: Proc SPIE Int Soc Optical Eng, SPIE, 5388: 167-178.

[2] Sobocinski M, Leinonen M, Juuti J and Jantunen H (2012) A piezoelectric active mirror suspension system embedded into low-temperature cofired ceramics, IEEE Transactions on Ultrasonics, Ferroelectrics and Frequency Control, 59 (9): 1990-1995.

[3] Niezrecki C, Brei D, Balakrishnan S and Moskalik A (2001) Piezoelectric actuation: state of the art. The Shock and Vibration Digest 33 (4): 269-280.

[4] Sheng W, Tiemin Z, Jiantao Z and Xiuli Y (2015) Optimal design of cymbal stack transducer in a piezoelectric linear actuator by finite element method. Energy Harvesting and Systems 2 (3-4): 169–176.

[5] Huan H, Gao C, Liu L, Sun Q, Zhao B and Yan L (2015) Research of ultrasound-mediated transdermal drug delivery system using cymbal-type piezoelectric composite transducer. International Journal of Thermophysics 36: 1312-1319.

[6] Narayanan M and Schwartz RW (2010) Design, fabrication and finite element modeling of a new wagon wheel flextensional transducer. Journal of electroceramics 24(3): 205–213.

[7] Ngernchuklin P, Eamchotchawalit C and Safari A (2015) Comparison of actuator performance in lead-based and lead-free piezoelectric cymbals, Joint IEEE International Symposium on the Applications of Ferroelectric (ISAF), International Symposium on Integrated Functionalities (ISIF), and Piezoelectric Force Microscopy Workshop (PFM), Singapore, 2015, 261-264.

[8] Poikselkä K, Leinonen M, Palosaari J, Vallivaara I, Haverinen J, Röning J and Juuti J (2016) End cap profile optimization of a piezoelectric Cymbal actuator for quasi-static operation by using a genetic algorithm, Journal of Intelligent Material Systems and Structures 27(4): 444-452.

[9] Codreanu I (2005) A parallel between differential evolution and genetic algorithms with exemplification in a microfluidics optimization problem. In: Proceedings of IEEE Semiconductor, International Conference, CAS 2005, 2: 421–424.

[10] Leu G, Simion S and Serbanescu A (2004) Mems optimization using genetic algorithms. In: Proceedings of IEEE Semiconductor, International Conference, CAS 2004, 2: 475–478.

[11] Darnobyt I, Kryvyy R, Lobur M and Tkatchenko S (2008) Possibilities of the use of genetic algorithms in design of mems elements. In: 2008 International Conference on Perspective Technologies and Methods in MEMS Design, 87.

[12] Hart GL, Blum V, Walorski MJ and Zunger A (2005) Evolutionary approach for determining first-principles hamiltonians. Nature materials 4(5): 391–394.

[13] Iwasaki T and Ikeda M (2001) Optimal design of flat structures for vibration suppression. In: Proceedings of the 2001 IEEE International Conference on Control Applications 2001, (CCA'01), 583–587.

[14] Chiu CW, Chao PC and Wu DY (2007) Optimal design of magnetically actuated optical image stabilizer mechanism for cameras in mobile phones via genetic algorithm. IEEE Transactions on Magnetics 43(6): 2582–2584.

[15] Susanto K and Yang B (2004) Genetic algorithm based optimization design of miniature piezoelectric forceps. In: IEEE International Conference on Robotics and Automation. ICRA'04. 2004, 2: 1358–1363.

[16] Lai YJ, Senesky DG and Pisano AP (2010) Genetic algorithm optimization for mems cantilevered piezoelectric energy harvesters. In: International Conference on Micro and Nanotechnology for Power Generation and Energy Conversion

Applications (PowerMEMS), 111–114.
[17] Chakraborti N (2004) Genetic algorithms in materials design and processing. International Materials Reviews 49(3-4): 246–260.
[18] Alibeigloo A, Shakeri M and Morowa A (2007) Optimal stacking sequence of laminated anisotropic cylindrical panel using genetic algorithm. Structural Engineering and Mechanics 25(6): 637–652.
[19] Ameri E, Aghdam M and Shakeri M (2012) Global optimization of laminated cylindrical panels based on fundamental natural frequency. Composite Structures 94(9): 2697–2705.
[20] Chang LK and Tsai MC (2014) Design of star-shaped flextensional stator for ultrasonic motor. Advances in Mechanical Engineering 6: 162535.
[21] Bruant I, Gallimard L and Nikoukar S (2010) Optimal piezoelectric actuator and sensor location for active vibration control, using genetic algorithm. Journal of sound and vibration 329(10): 1615–1635.
[22] Saxena A (2005) Topology design of large displacement compliant mechanisms with multiple materials and multiple output ports. Structural and Multidisciplinary Optimization 30(6): 477–490.
[23] Li X, Shih WY, Vartuli JS, Milius DL, Aksay IA and Shih W-H (2002) Effect of a transverse tensile stress on the electric-field-induced domain reorientation in soft PZT: in situ XRD study. Journal of the American Ceramic Society 86(4): 844–850.